Martin Köchy

Stochastic time series of daily precipitation for the interior of Israel

first published in:
Israel Journal of Earth Science - 55 (2006), 2, p. 103-109
ISSN: 0021-2164
DOI: 10.1560/IJES_55_2_103

Postprint published at the institutional repository of Potsdam University:
In: Postprints der Universität Potsdam :
Mathematisch-Naturwissenschaftliche Reihe ; 29
http://opus.kobv.de/ubp/volltexte/2007/1315/
http://nbn-resolving.de/urn:nbn:de:kobv:517-opus-13155

Published in *Israel Journal of Earth Science* 55:103-109, doi: 10.1560/IJES_55_2_103
available at http://www.sciencefromisrael.com/

Stochastic time series of daily precipitation for the interior of Israel

(Short contribution)

Martin Köchy

Research group Plant ecology and nature conservation

Maulbeerallee 3

Potsdam University

Postfach 60 15 53

14415 Potsdam

GERMANY

Telephone: +49-331-977 1974

Telefax: +49-331-977 1948

E-mail: martin.koechy@gmx.net

Running head: Stochastic time series of precipitation

Abstract

This contribution describes a generator of stochastic time series of daily precipitation for the interior of Israel from c. 90 to 900 mm mean annual precipitation (MAP) as a tool for studies of daily rain variability. The probability of rainfall on a given day of the year is described by a regular Gaussian peak curve function. The amount of rain is drawn randomly from an exponential distribution whose mean is the daily mean rain amount (averaged across years for each day of the year) described by a flattened Gaussian peak curve. Parameters for the curves have been calculated from monthly aggregated, long-term rain records from seven meteorological stations. Parameters for arbitrary points on the MAP gradient are calculated from a regression equation with MAP as the only independent variable. The simple structure of the generator allows it to produce time series with daily rain patterns that are projected under climate change scenarios and simultaneously control MAP. Increasing within-year variability of daily precipitation amounts also increases among-year variability of MAP as predicted by global circulation models. Thus, the time series incorporate important characteristics for climate change research and represent a flexible tool for simulations of daily vegetation or surface hydrology dynamics.

Introduction

Projections of the effect of climate change on crops, natural vegetation, and surface hydrological processes usually rely on simulations of future climates. In arid to Mediterranean climates like Israel's, changes in precipitation may be more important than changes in temperature. Global circulation models generally project an increase in extreme precipitation events and greater variability both within and among years (Easterling et al., 2000). This is supported by changes in historic regional climate records (e.g. Ben-Gai et al., 1998; Alpert et al., 2002). Changes in the distribution of daily rain patterns have significant direct impacts on hydrological and ecological processes (Weltzin et al., 2003; Loik et al., 2004) including runoff, erosion, groundwater recharge, vegetation productivity, decomposition, and ecosystem stability with repercussions for the socio-economic framework of millions of humans (Milliman et al., 1992). Global and regional projections of climate change and its impact on the environment still include some uncertainty (Watson et al., 1997). Projections of climate change for Israel are still more uncertain than those for other countries because of Israel's small size compared to the grid cell size of most current global circulation models (Pe'er and Safriel, 2000). The uncertainty of the extent of climate change in Israel is surpassed by that of projections of socioeconomic changes (Milliman et al., 1992; Pe'er and Safriel, 2000), although a comprehensive multi-disciplinary project is underway to remedy this situation (Hoff et al., 2006). For simulations of future changes in hydrology and ecology modellers prefer stochastic time series of precipitation to static time slices

58 for incorporating and assessing the variability of climate on environmental
59 processes (Srikanthan and McMahon, 2001). Only two generators of stochastic
60 time series for Israel have been described so far. These are specific to the Tel-Aviv
61 area (Gabriel and Neuman, 1962) and the Arava (Barzilay et al., 2000). Other,
62 more general generators of stochastic time series (Srikanthan and McMahon,
63 2001) require the calibration of many parameters (e.g. 48, Wilks, 1992) and are
64 therefore not easily adapted to other regions or to include changes in rain intensity
65 or frequency as observed in the past (Alpert et al., 2002) or projected by global
66 circulation models (Easterling et al., 2000). Here I present ReGen, a generator of
67 stochastic time series of daily precipitation for sites in the interior of Israel with 90
68 to 900 mm mean annual precipitation. Additionally, the generator allows the
69 manipulation of daily rain patterns (intensity and frequency) as projected by global
70 circulation models.

71 # Methods

72 The ReGen simulator produces stochastic time series of daily precipitation for
73 locations along a transect from the northern edge of the Negev desert to the
74 Galilee mountains in Israel (90 to 900 mm mean annual precipitation, elevation 300
75 – 500 m). The distribution of rainy days in the region is unimodal as a first
76 approximation (Goldreich 1995). The time series are generated by a so-called two-
77 part model (Srikanthan and McMahon 2001). The first part is a regular bell-shaped
78 seasonal function (Gaussian peak curve). It determines the daily probability, p_d,
79 that a given *day* of the year is a rainy day as

$p_d = amplitude \cdot \mathbf{exp}[-(day - location)^{shape} / (2 \cdot width^2)]$,

where *shape* = 2, and day 1 = August 1 (Fig. 1a). Counting the days from August 1 centres the distributions conveniently and corresponds to the traditional "rainfall year" (Goldreich, 1995). The curve becomes periodic by the function *day* := (*day* + 182 – *location*) **mod** 365 – 182 + *day*. I specified a minimum probability threshold of 0.05 for rainfall to avoid unrealistic rain events in summer. The second part of the model is a similar bell-shaped seasonal function with *shape* = 4 to produce a flattened curve (Fig. 1b). This function determines the daily mean rain amount DMR_d, i.e., the rain amount for a given day of the year averaged across years. The rain amount for a specific rainy day is drawn randomly from an exponential distribution whose mean corresponds to DMR_d. The distribution has the advantage of requiring only one parameter, but it under-represents the frequency of rain categories <5 mm. This decreases the length of rain spells according to their definition as consecutive rains with >0.1 mm rain (e.g., Paz and Kutiel, 2003), but it has few consequences for the practical application of ReGen because the volumes involved are so small. The three parameters (except *shape*) of each of the two Gaussian peak curves were determined by nonlinear regression of monthly aggregated long-term data from seven meteorological stations along a MAP gradient in the interior of Israel (Tab. 1). I excluded from the data days with rain <0.5 mm and set rain amount = 0 for months with ≤2 rainy days summed across years. The historic precipitation records of the seven stations along the MAP gradient showed no significant autocorrelation (Durbin-Watson test). Therefore, I did not introduce any annual autocorrelation in the stochastic time series either.

The non-linear regressions of *p* and DMR explained ≥89% of the monthly variation at each station.

For generating stochastic time series of daily precipitation for arbitrary values of MAP between 90 and 900 mm, I calculated regressions of each parameter of the two Gaussian peak curves (except *shape*) on MAP. *Amplitude* and *width* of precipitation likelihood and *amplitude* of DMR could be predicted well by MAP (Tab. 2). For the other three (*location* of the maximum of precipitation likelihood, *location* of the maximum of daily mean amount, and *width* of daily mean amount) the slope of the regression was not significantly different from zero so I used their means. The model structure allows the mid-season date to be changed without affecting MAP by adjusting the *location* parameters (Fig. 1). Adjusting the *width* parameters changes the average length of the rainy season. Increasing the *amplitude* parameters increases rain frequency and intensity.

Manipulation of daily rain pattern

In order to study the shift in daily rain amount distribution to more rainstorms, the amplitude of DMR can be adjusted by up to ±30% (ΔDMR) in ReGen. For comparison, the RegCM3 global circulation model with a resolution of 0.5° × 0.5° projects for the pessimistic A2 climate change scenario an average increase in DMR of 3% for Israel North of the Negev desert while it projects an average increase in DMR of 29% (derived from Giorgi et al., 2004a, b) for the optimistic B2 scenario. In order to keep MAP the same, a change of DMR is compensated for by decreasing the amplitude of daily mean rain probability (*p*) using the empirically

derived equation $p^* = p \cdot [1 - C + 1.33 \cdot C^2 - (0.61 + 1.57 \cdot p) \cdot C^3)$, where C is the relative change in DMR (ΔDMR/100). Thus, increasing DMR reduces the frequency of days with light rain and lengthens the intervals between them. On the other hand, it increases the frequency of rainstorms and shortens the intervals between them.

Statistical analyses

I compared MAP, mean number of days with ≥5, ≥15, and ≥25 mm precipitation, and intervals between days ≥5, ≥15, and ≥25 mm precipitation between simulated (30 yr) and observed time series using 95% confidence intervals (CI). These comparisons comprised the seven stations used to calculate the regression parameters and ten other stations (Tab. 1). Further, I used 95%-CIs to compare the effect of increasing DMR by –20, –10, 0, +10, and +20% on the mean number of days with ≥5, ≥15, and ≥25 mm precipitation and mean intervals between them at five points (100, 300, 450, 600, and 800 mm) on the MAP gradient. Finally, I used a multiple regression to compare the effect of change of DMR on the coefficient of variation (CV) of annual rain amount along the MAP gradient.

Results and Discussion

The rain pattern of a single 30-yr stochastic time series, with only the mean annual precipitation of each climate station as input to ReGen, was compared to historic climate records. MAP and mean number of days with daily rain amounts ≥5, ≥15, and ≥25 mm did not differ significantly between simulated and observed time series for most stations (Figs. 2, 3). In the same way, intervals between days

146 with rain amounts ≥5, ≥15, and ≥25 mm were similar in simulated and observed
147 time series in most cases (data not shown). Although ReGen was parameterized
148 with data from meteorological stations in the interior of Israel, its time series also
149 reproduced the characteristics of historic data from stations outside of this area
150 well (Figs. 2, 3). ReGen is also capable of reproducing the "median dates of
151 accumulated percentage of the annual rainfall" and thus the "median rainy season
152 length" using the approach of Paz and Kutiel (2003), albeit with a shift of the
153 median dates by up to one week which is imposed by the fixed *location*
154 parameters.
155 The CV of simulated MAP (19%) was significantly smaller than that of observed
156 time series (33%). The lower CV in simulations was due to a more normal
157 distribution of annual precipitation values than observed in nature (Ben-Gai et al.,
158 1998). Thus, the time series do not include years with extreme annual precipitation
159 amounts. This can be easily amended in long-term simulations by specifying an
160 annually variable MAP input to ReGen according to observed or projected
161 distributions of annual rain amounts (Ben-Gai et al., 1998).
162 Increasing DMR decreased strongly the average number of days with ≥5 mm of
163 rain, increased markedly the number of days with ≥15 mm, and increased slightly
164 days with ≥ 25 mm of rain (Fig. 4a). Correspondingly, the median interval between
165 days with ≥5 mm rain increased, but the interval between days with ≥15 and ≥25
166 mm of rain decreased (Fig. 4b). Thus, heavy rainfalls contributed more and light
167 rainfall less to annual precipitation than under current conditions (Fig. 5) as
168 intended by the manipulation of the daily rain pattern. This is in line with

observations of shifts of rain distribution in the Mediterranean (Alpert et al., 2002). Increasing DMR also had an effect on annual rain characteristics. It increased the CV of annual precipitation (AP), independent of MAP, by 10% ($CV_{AP} = 29 – 0.018 \cdot MAP + 0.1 \cdot \Delta DMR$; $R_a^2 = 0.72$, $F_{2,22} = 32$; the interaction between the two variables was not significant). Thus, the model confirms observations and simulations that the frequency of extreme events within a year is linked to the frequency of extreme years on the decadal time scale (Easterling et al., 2000).

The time series produced by ReGen are based on a unimodal distribution of rainy days because the original data were aggregated by months which smoothes the secondary and tertiary peaks of the actual multimodal distribution (Goldreich, 1995; Osetinsky and Alpert, 2006). Although the periodicity of the synoptic systems causing the higher-level peaks and their average dates are known (Osetinsky and Alpert, 2006), their relative contribution to the total precipitation volume and relative temporal shift among each other has yet to be determined along the aridity gradient. In addition, the more faithful reproduction of actual rain patterns would reduce the flexibility and generality of the ReGen model.

In summary, ReGen can generate daily time series with quasi-realistic characteristics based on a single input variable, MAP. The algorithm can be applied to a large part of Israel without modification. Changes in daily rainfall frequency distribution as projected by global circulation models are incorporated through one additional input variable. Thus, ReGen is a flexible tool for studying the effect of daily rain patterns on the environment in Israel under current and under climate change conditions.

Acknowledgements

I thank P. Alpert, S.O. Krichak, M. Dayan, and I. Osetinsky for processing the RegCM3 data. Precipitation data was obtained from the Israel Meteorological Service and the Royal Netherlands Meteorological Institute (KNMI). P. Suppan and two anonymous reviewers critically commented on early versions of the manuscript. This contribution is part of the GLOWA Jordan River project funded by BMBF, the German Federal Ministry of Education and Research, contract 01LW0306(A). The author alone is responsible for the content of this publication.

References

Alpert, P., Ben-Gai, T., Baharad, A., Benjamini, Y., Yekutielli, D., Colacino, M. 2002. The paradoxical increase of Mediterranean extreme daily rainfall in spite of decrease in total values. Geophysical Research Letters 29: 31.1-31.4.

Barzilay, E., Enzel, Y., Amit, R. Hassan, M. A., Slaymaker, O., Berkowicz, S. M., eds. 2000. Constructing synthetic time series of rainfall events for a hyperarid environment, southern Arava, Israel. IAHS Publication 261. International Association of Hydrological Sciences.

Ben-Gai, T., Bitan, A., Manes, A., Alpert, P., Rubin, S. 1998. Spatial and temporal changes in rainfall frequency distribution patterns in Israel. Theoretical and Applied Climatology 61: 177-190.

Easterling, D. R., Meehl, G. A., Parmesan, C., Changnon, S. A., Karl, T. R., Mearns, L. O. 2000. Climate extremes:observations, modelling, and impacts. Science 289: 2068-2074.

Gabriel, K. R., Neuman, J. 1962. A Markov chain model for daily rainfall at Tel Aviv. Quarterly Journal of the Royal Meteorological Society 88: 90-95.

216 Giorgi, F., Bi, X., Pal, J. 2004a. Mean, interannual variability and trends in a
217 regional climate change experiment over Europe. II: climate change scenarios
218 (2071-2100). Climate Dynamics 23: 839-858.
219 Giorgi, F., Bi, X., Pal, J. S. 2004b. Mean, interannual variability and trends in a
220 regional climate change experiment over Europe. I. Present-day climate
221 (1961-1990). Climate Dynamics 22: 733-756.
222 Goldreich, Y. 1995. Temporal variations of rainfall in Israel. Climate Research 5:
223 167-179.
224 Hoff, H., Küchmeister, H., Tielbörger, K. 2006. The GLOWA Jordan River Project –
225 Integrated Research for Sustainable Water Management. Beck, M. B.,
226 Speers, A. eds. 2nd IWA Leading-Edge Conference on Sustainability in
227 Water-Limited Environments, Sydney, Australia, November 2004. IWA Water
228 and Environment Management Series Vol. 10. London: IWA Publishing; pp.
229 73-80.
230 Loik, M. E., Breshears, D. D., Lauenroth, W. K., Belnap, J. 2004. A multi-scale
231 perspective of water pulses in dryland ecosystems: climatology and
232 ecohydrology of the western USA. Oecologia 141: 269-281.
233 Milliman, J. D., Jeftić, L., Sestini, G. 1992. The Mediterranean Sea and climate
234 change — An overview. Jeftic, L., Milliman, J. D., Sestini, G. eds. Climatic
235 change and the Mediterranean. Vol. 1. London: E. Arnold; pp. 1-14.
236 Osetinsky, I., Alpert, P. 2006. Calendaricities and multimodality in the Eastern
237 Mediterranean cyclonic activity. Natural Hazards and Earth System Sciences
238 6: 587-596.
239 Paz, S., Kutiel, H. 2003. Rainfall regime uncertainty (RRU) in an Eastern
240 Mediterranean region — A methodological approach. Israel Journal of Earth
241 Sciences 52: 47-63.
242 Pe'er, G., Safriel, U. N. 2000. Climate change: Israel national report under the
243 United Nations Framework Convention on Climate Change: Impact,
244 vulnerability and adaptation. http://www.bgu.ac.il/BIDR/rio/Global91-
245 editedfinal.html (viewed 2004-11-04).

246 Srikanthan, R., McMahon, T. A. 2001. Stochastic generation of annual, monthly
247 and daily climate data: A review. Hydrology and Earth System Sciences 5:
248 653-670.
249 Watson, R. T., Zimyowera, M. C., Moss, R. H., Dokken, D. J., eds. 1997. The
250 regional impacts of climate change: an assessment of vulnerability. Summary
251 for policymakers. Cambridge: Cambridge University Press.
252 Weltzin, J. F., Loik, M. E., Schwinning, S., Williams, D. G., Fay, P. A., Haddad, B.
253 M. 2003. Assessing the response of terrestrial ecosystems to potential
254 changes in precipitation. Bioscience 53: 941-952.
255 Wilks, D. S. 1992. Adapting stochastic weather generation algorithms for climate
256 change studies. Climatic Change 22: 67-84.
257
258

Appendix

Script for use with the statistical program *R* (R Development Core Team. 2005. R: A language and environment for statistical computing. R Foundation for Statistical Computing, Vienna, Austria. ISBN 3-900051-07-0, URL http://www.R-project.org.). Code for c++ can be obtained from the author.

```
# Gauss peak curve function for calculating daily precipitation
# probability and mean rain volume
# numbering of days begins with August 1 = 1
gauss <- function (day, amplitude, location, width, shape=2)
{    day = (day + 182 - location) %% 365 + location - 182
     G = amplitude*exp(-(day-location)^shape/(2*width^2))
     return(G)
}

# Calculation of parameters based on mean annual precipitation
# and change of daily mean rain (relCh)
rmp<-function (MAP, relCh=0)
{    H = 0.13 + 0.00041 * MAP # rain occurance
     H = H*(1-relCh +1.33*relCh^2-(0.61+1.57*H)*relCh^3)
     X = 177
     W = 52 + 0.007 * MAP
     h = -14 + 4 * log(MAP) # rain volume
     h = h * (1+relCh)
     x = 170
     w = 10488
     return(data.frame(RH=H,RX=X,RW=W,Vh=h,Vx=x,Vw=w)
}

############# Production of stochastic time series ###############
# Parameters can be entered directly or as 'scenario' calculated #
# by function 'rmp'                                              #

ReGen<-function (years, amplitudeR=0, locationR=0, widthR=0, amplitudeV=0,
locationV=0, widthV=0, scenario=0)
{    DM = matrix(rep(1:365, years),nrow=years, byrow=T)
     if(sum(scenario)>0)
     {    amplitudeR=as.numeric(scenario[1])
          locationR=as.numeric(scenario[2])
          widthR=as.numeric(scenario[3])
          amplitudeV=as.numeric(scenario[4])
          locationV=as.numeric(scenario[5])
          widthV=as.numeric(scenario[6])
     }

     # probability of a rainy day
```

```
304         G<-gauss(DM, amplitudeR, locationR, widthR)
305         RT<-ifelse(runif(DM)<G & G>0.05, 1, 0)
306         # daily mean rain volume:
307         RV<- gauss(DM, amplitudeV, locationV, widthV, 4)
308         # actual rain volume:
309         R<- RT * rexp(DM, 1/RV)
310         return(R)
311     }
312
```

Tables

Table 1. Details of climate stations from which data were used for the derivation of model parameters and for validation (Figs. 2, 3).

Station	MAP (mm)	Longitude (° E)	Latitude (° N)	Years
parameterization				
Beer Sheva	196	34.78	31.23	1957–2000
Bet Guvrin	395	34.90	31.62	1950–2000
Bet Meir	626	35.03	31.80	1977–2000
Elon	813	35.22	33.05	1974–2000
HarKnaan	717	35.50	32.97	1949–1998
Rosh Zurim	567	34.79	30.87	1983–2000
Sede Boqer	90	35.45	33.07	1952–2000
validation				
Dorot	371	34.63	31.50	1950–2000
Haifa Bay	561	35.03	32.80	1987–1999
Jerusalem	591	35.22	31.77	1967–1999
Kebutzat Kinneret	400	35.61	33.17	1949–2001
Kefar Blum	506	35.57	33.25	1949–2001
Kefar Giladi	767	34.72	31.27	1949–2001
Nahal Hatzerim	170	35.12	31.80	1967–1999
Qiryat Anavim	692	34.82	32.12	1950–2000
Qiryat Shaul	549	35.13	31.66	1949–2000
Yiron	739	35.57	32.72	1949-2001

317 Table 2. Predictors for parameters used in stochastic time series of daily

318 precipitation (MAP: mean annual precipitation; day 1 = August 1).

parameter	**equation**	R^2
likelihood		
amplitude	0.13 + 0.00041 MAP	0.98
location of maximum (day)	177	
width (days)	52 + 0.007 MAP	0.82
volume		
amplitude (mm)	–14 + 4 ln(MAP)	0.85
location of maximum (day)	170	
width (days)	10488	

319

320

Figures

Fig. 1. Gaussian peak curves for the daily probability of rainy days (a) and the daily mean rain amount (b) of a site with 450 mm MAP. b = [8 · (*shape* – 1) / *shape*]$^{-0.5}$

Fig. 2. Deviation of simulated from observed mean annual precipitation (ΔMAP, dashes with vertical bars indicating the mean ± 95%-confidence interval). Thin, continuous lines connect the 95%-confidence intervals of observed MAP.

Fig. 3. Comparison of rain pattern in exemplary 30-yr time-series (outline symbols) generated by the ReGen model (Tab. 2) with that of historic rain data (filled symbols; Tab. 1). Error bars indicate 95%-confidence intervals. Thresholds: squares: 5 mm, diamonds: 15 mm, circles: 25 mm.

Fig. 4. Effect of changing the amplitude of daily mean precipitation on rain pattern in single 150-yr stochastic time series. a) mean annual number of days with total rain amount ≥5 mm (squares), ≥15 mm (diamonds), and ≥25 mm (circles) and 20% higher amplitude (dotted), 20% lower amplitude (dashed), and unchanged (continuous line). b) mean of annual median intervals between days with ≥5, ≥15, and ≥25 rain amount on a logarithmic scale (symbols as in left panel). Error bars indicate 95%-confidence intervals (CI). CIs in the left panel are ≤ symbol size.

Fig. 5. Exemplary effect of changing daily mean rain amount by +20% (dashed line), 0% (continuous line), or –20% (dotted line) on the relative contribution of daily amount categories (averaged across 30 years) to annual precipitation for 450 mm MAP.

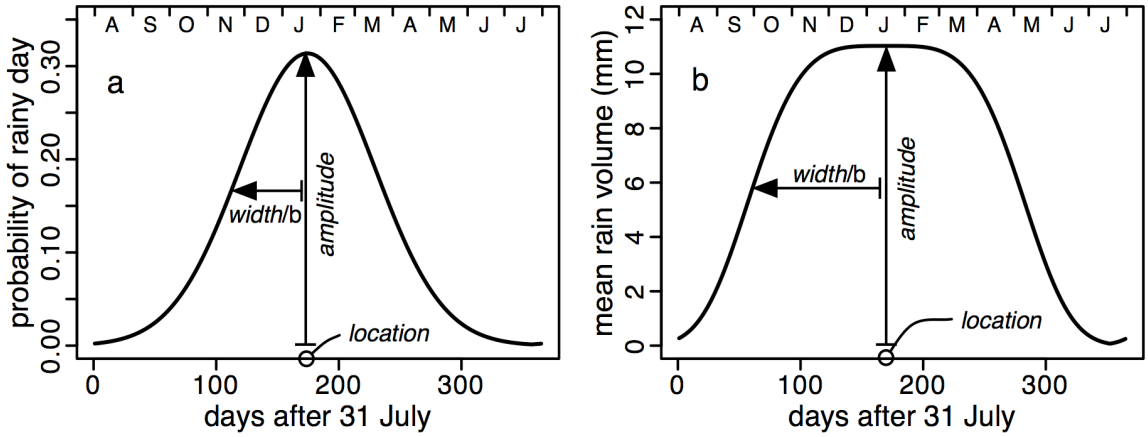

342

343 Fig. 1. Gaussian peak curves for the daily probability of rainy days (a) and the daily mean rain

344 amount (b) of a site with 450 mm MAP. b = $[8 \cdot (shape - 1) / shape]^{0.5}$

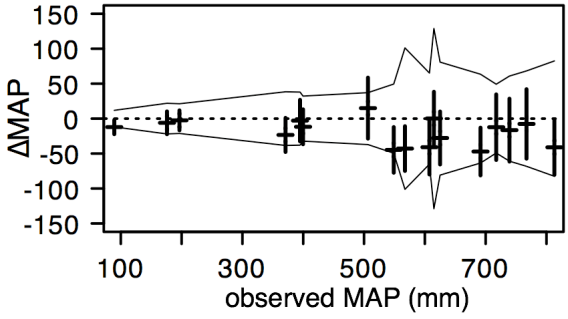

345

346 Fig. 2. Deviation of simulated (30 yr) from observed mean annual precipitation (ΔMAP, dashes with

347 vertical bars indicating the mean ± 95%-confidence interval) for stations in Tab. 1. Thin, continuous

348 lines connect the 95%-confidence intervals of observed MAP.

349

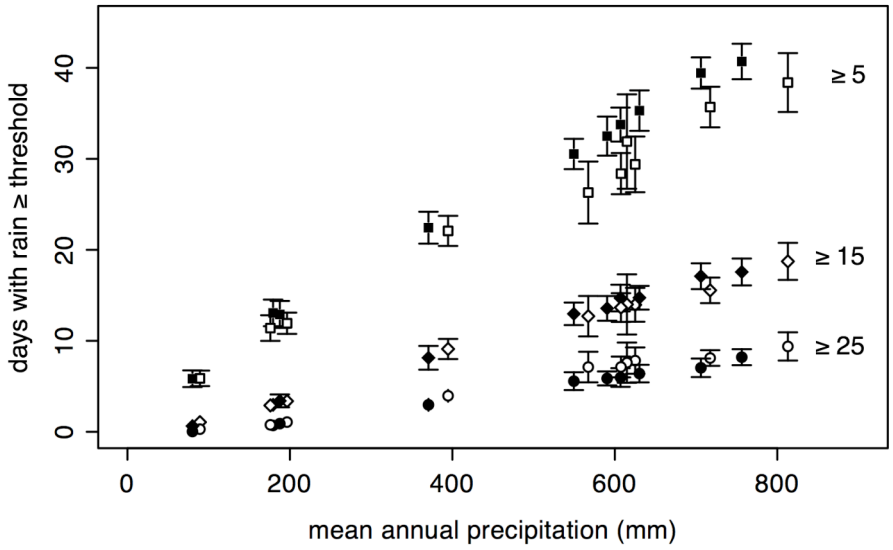

Fig. 3. Comparison of rain pattern in exemplary 30-yr time-series (outline symbols) generated by the ReGen model (Tab. 2) with that of historic rain data (filled symbols; Tab. 1). Error bars indicate 95%-confidence intervals. Thresholds: squares: 5 mm, diamonds: 15 mm, circles: 25 mm.

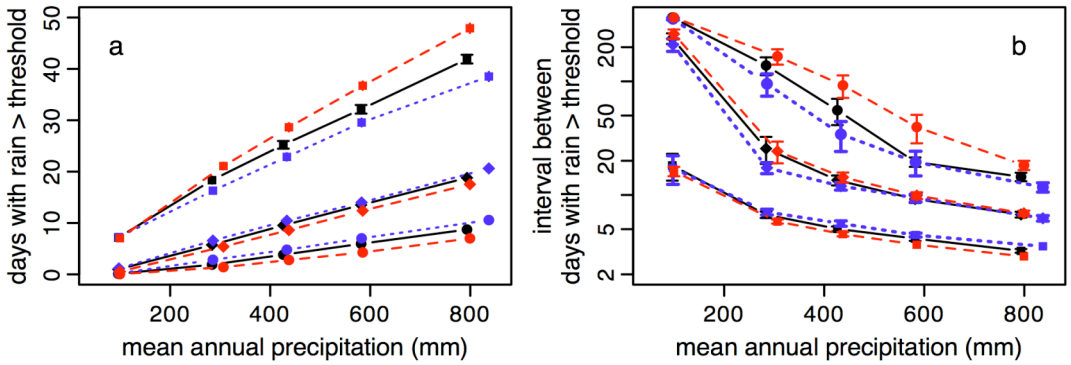

Fig. 4. Effect of changing the amplitude of daily mean precipitation on rain pattern in single 150-yr stochastic time series. a) mean annual number of days with total rain amount ≥5 mm (squares), ≥15 mm (diamonds), and ≥25 mm (circles) and 20% higher amplitude (dotted), 20% lower amplitude (dashed), and unchanged amplitude (continuous line). b) mean of annual median intervals between days with ≥5, ≥15, and ≥25 rain amount on a logarithmic scale (symbols as in left panel). Error bars indicate 95%-confidence intervals (CI). CIs in the left panel are ≤ symbol size.

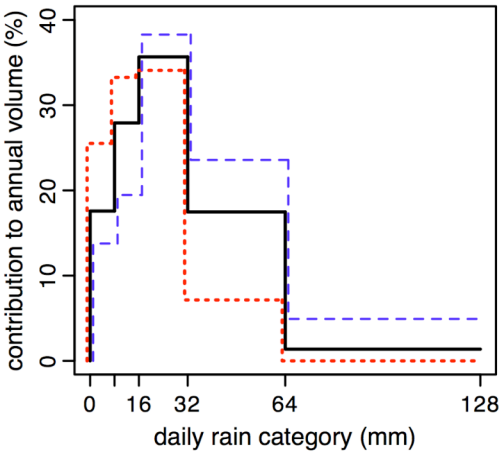

363

364 Fig. 5. Exemplary effect of changing daily mean rain amount by +20% (dashed line), 0%

365 (continuous line), or –20% (dotted line) on the relative contribution of daily amount categories

366 (averaged across 30 years) to annual precipitation for 450 mm MAP.